PREDICTIVE CONTROL OF A MAGNETIC LEVITATION SYSTEM WITH INFEASIBILITY HANDLING BY RELAXATION OF OUTPUT CONSTRAINTS

Rubens Junqueira Magalhães Afonso, rubensjma@gmail.com
Roberto Kawakami Harrop Galvão, kawakami@ita.br
Instituto Tecnológico de Aeronáutica, Divisão de Engenharia Eletrônica, 12228-900, São José dos Campos - SP

Abstract. This paper investigates the potential benefits of using an appropriate infeasibility handling scheme for the constrained predictive control of a magnetic levitation system. In this case, the input constraints are related to physical limits on the intensity and rate of variation of the current applied to the electromagnet coil. The output constraints refer to the width of the air gap between the electromagnet core and the suspended object, which should be kept within proper operational limits. Infeasibility may arise, for instance, because of modelling errors and sensor noise. In order to circumvent such difficulties, the technique adopted in this work allows a progressive relaxation of the upper and lower output constraints in the entire prediction horizon until the resulting quadratic programming problem becomes feasible. Results obtained by simulation show that such a relaxation procedure leads to an appropriate recovery from constraint violations. Moreover, it also circumvents infeasibility problems associated to future violations, which may be caused by incorrect predictions. In this case, because of the receding horizon implementation of the controller, such violations may actually be avoided. The results are compared to those obtained by using a standard quadratic programming implementation, which minimizes the distance between the compromise solution and the feasibility boundary, if a feasible solution cannot be found. It is shown that such an alternative may actually fail to maintain closed-loop stability.

Keywords: magnetic levitation, predictive control, infeasibility handling, constraint relaxation.

1. Introduction

The importance of magnetic levitation (maglev) technology has been increasing in a significant manner in the recent past. Growing interest in this technology can be found in a wide range of fields, with applications including, for instance, photolithography devices for semiconductor manufacturing (Kim and Trumper 1998), high-speed transportation systems (Holmer 2003), seismic attenuators for gravitational wave antennas (Varvella *et al.* 2004) and self-bearing blood pumps (Masuzawa *et al.* 2003) for use in artificial hearts.

It is indispensable to keep most maglev systems working under tight constraints to ensure good energy conversion performance. In addition, failure to enforce such constraints may lead to catastrophic faults, since the magnetic force may not be strong enough to bring the object back to its reference position. Moreover, the current at the electromagnet coil is usually subject to slew rate and amplitude limitations, which places a constraint on the control variables. Therefore, the natural handling of constraints presented by Model Predictive Control (MPC) implementations arises as an interesting approach to this problem, as discussed in (Fama *et al.* 2005).

In the context of MPC, infeasibility handling becomes an important issue because external perturbations, measurement noise, modelling errors, among other factors, may make it impossible to respect all the constraints (Maciejowski 2002). In this case, the use of an infeasibility handling technique is vital to bring the system back to a feasible region in a graceful manner. However, it is often not obvious which constraints to relax and the amount by which they should be relaxed in order to attain a feasible optimization problem.

In this work, the benefits of a progressive relaxation of output constraints for the operation of a single-axis, attractive maglev system under MPC control are studied. A standard solution provided by the Matlab `quadprog` function, which minimizes the distance between the compromise solution and the feasibility boundary, is used for comparison.

The remaining sections are organized as follows. The adopted MPC formulation and the controller equations are described in Section 2. In Section 3, some of the main infeasibility handling approaches are discussed and the technique under study is detailed. Section 4 describes the simulation model of the maglev system considered in this work, as well as the linearized model used in the predictive control law and the simulation scenarios employed in the investigation. Section 5 presents the results obtained with the constraint relaxation method under consideration, as well as with the default infeasibility handling approach provided by Matlab. Finally, concluding remarks are given in Section 6.

2. Predictive control formulation

Figure 1 presents the main elements of the discrete-time predictive control formulation adopted in this work. A plant model is employed to calculate output predictions up to N steps in the future, where N is termed "Prediction Horizon". Such predictions are determined on the basis of the state measured at the present time (k^{th} sampling instant), and are also dependent on the control sequence that will be applied.
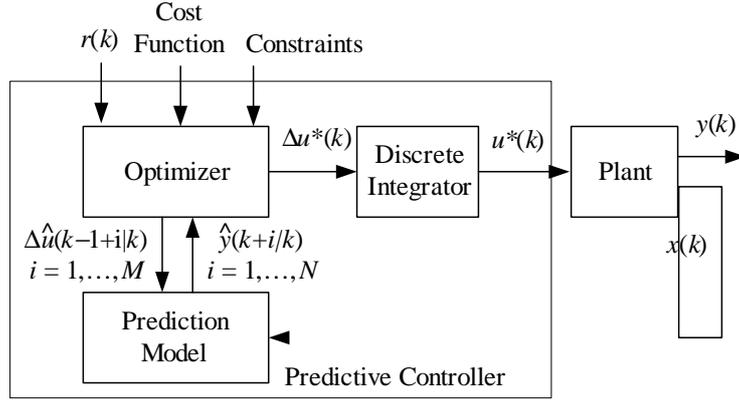
Figure 1. Predictive control loop employing state feedback. The optimal control at instant k is denoted by $u^*(k)$.

In the mathematical formulation presented below, the following notation is adopted. The controlled (plant output), manipulated (plant input), reference and state variables at the kth sampling instant are denoted by $y(k) \in \mathbb{R}$, $u(k) \in \mathbb{R}$, $r(k) \in \mathbb{R}$, $x(k) \in \mathbb{R}^n$, respectively. Increments are denoted by $\Delta y(k) = y(k) - y(k-1)$. The hat symbol (ˆ) denotes a predicted value. Reference and predicted values are stacked in column vectors as

$$R = \begin{bmatrix} r(k+1) \\ \vdots \\ r(k+N) \end{bmatrix}, \quad \hat{Y} = \begin{bmatrix} \hat{y}(k+1|k) \\ \vdots \\ \hat{y}(k+N|k) \end{bmatrix}, \quad \Delta\hat{U} = \begin{bmatrix} \Delta\hat{u}(k+1|k) \\ \vdots \\ \Delta\hat{u}(k+M|k) \end{bmatrix} \tag{1}$$

where N and M are the prediction and control horizons, respectively. Finally, T_N, I_N and Γ_N denote a $N \times N$ lower triangular matrix of ones, a $N \times N$ identity matrix, and a $N \times 1$ column vector of ones, respectively.

The optimizer depicted in Fig. 1 determines the sequence of future control increments $\Delta\hat{u}(k-1+i|k), i = 1, \ldots, M$ that minimizes the cost function specified for the problem, subject to constraints on the plant inputs and outputs. The value of M ("Control Horizon") is typically smaller than N, and the optimization assumes that $\Delta\hat{u}(k-1+i|k) = 0$ for $M < i \leq N$. The control is implemented in a receding horizon manner, that is, only the first element of the optimized control sequence is applied to the plant and the optimization is repeated at the next sampling instant, on the basis of fresh measurements.

The following cost function, which penalizes tracking errors at the plant output and control variations at the plant input, was adopted:

$$J(\Delta\hat{U}) = \sum_{i=1}^{N}[\hat{y}(k+i|k) - r(k+i)]^2 + \sum_{i=1}^{M}\rho[\Delta\hat{u}(k-1+i|k)]^2 \tag{2}$$

where $\rho > 0$ is a weight parameter that can be used to tune the performance of the control loop. Using vector-matrix notation, the cost function can be rewritten in the form

$$J(\Delta\hat{U}) = (\hat{Y} - R)^T(\hat{Y} - R) + \rho\Delta\hat{U}^T\Delta\hat{U} \tag{3}$$

The relation between $\hat{Y}$ and $\Delta\hat{U}$ can be expressed by a prediction equation based on an incremental state-space model. By assuming a linearized model of the form $x(k+1) = Ax(k) + Bu(k)$, $y(k) = Cx(k)$, the incremental model can be written as $\Delta x(k+1) = A\Delta x(k) + B\Delta u(k)$, $\Delta y(k) = C\Delta x(k)$. Therefore, a prediction equation for Δy can be written as (Maciejowski 2002)

$$\Delta\hat{Y} = \underbrace{\begin{bmatrix} CB & 0 & \cdots & 0 \\ CAB & CB & \cdots & 0 \\ \vdots & \vdots & \ddots & \vdots \\ CA^{N-1}B & CA^{N-2}B & \cdots & CA^{N-M}B \end{bmatrix}}_{P} \Delta\hat{U} + \underbrace{\begin{bmatrix} CA \\ CA^2 \\ \vdots \\ CA^N \end{bmatrix}}_{Q} \Delta x(k) = P\Delta\hat{U} + Q\Delta x(k) \tag{4}$$

It can be easily seen that $\Delta\hat{Y}$ and $\hat{Y}$ are related as

$$\hat{Y} = \begin{bmatrix} 1 & 0 & \cdots & 0 \\ 1 & 1 & \cdots & 0 \\ \vdots & \vdots & \ddots & \vdots \\ 1 & 1 & 1 & 1 \end{bmatrix} \Delta\hat{Y} + \begin{bmatrix} 1 \\ 1 \\ \vdots \\ 1 \end{bmatrix} y(k) \tag{5}$$

or $\hat{Y} = T_N \Delta \hat{Y} + \Gamma_N y(k)$. Moreover, by using (4), it follows that

$$\hat{Y} = \underbrace{T_N P}_{G} \Delta \hat{U} + \underbrace{T_N Q \Delta x(k) + \Gamma_N y(k)}_{F} = G \Delta \hat{U} + F. \tag{6}$$

Therefore, the cost function (3) can be rewritten as

$$
\begin{aligned}
J(\Delta \hat{U}) &= (G \Delta \hat{U} + F - R)^T (G \Delta \hat{U} + F - R) + \rho \Delta \hat{U}^T \Delta \hat{U} & (7)\\
&= \Delta \hat{U}^T (G^T G + \rho I_M) \Delta \hat{U} + 2(F - R)^T G \Delta \hat{U} + (F - R)^T (F - R) & (8)
\end{aligned}
$$

which is quadratic in $\Delta \hat{U}$.

If restrictions on the manipulated and controlled variables of the form $u_{min} \le \hat{u}(k-1+i|k) \le u_{max}$, $i = 1, \ldots, M$ and $y_{min} \le \hat{y}(k+i|k) \le y_{max}$, $i = 1, \ldots, N$, are to be satisfied, the minimization of the cost is subject to the following linear constraints on $\Delta \hat{U}$ (Camacho and Bordons 1999):

$$
\begin{bmatrix} T_M \\ -T_M \\ G \\ -G \end{bmatrix} \Delta \hat{U} \le \begin{bmatrix} Bl_M[u_{max} - u(k-1)] \\ Bl_M[u(k-1) - u_{min}] \\ Bl_N[y_{max}] - F \\ F - Bl_N[y_{min}] \end{bmatrix} \tag{9}
$$

where $Bl_N[\bullet]$ is an operator that stacks N copies of a given column vector. The set of constraints (9) can be rewritten in compact form as $S \Delta \hat{U} \le b$. Therefore, the optimization problem to be solved at each sampling period is one of Quadratic Programming (quadratic cost, linear constraints), for which efficient numerical algorithms are available (Maciejowski 2002).

It is worth noting that the formulation presented above has inherent integral control action, as can be seen from the presence of a discrete integrator in fig. 1. Such a feature stems from the use of an incremental state-space model. In this sense, the present formulation is more elegant than the version employed in (Fama *et al.* 2005).

3. Constraint relaxation approaches

As mentioned in Section 1, it is not always possible to enforce all constraints because the effects of measurement noise, external disturbances and modelling errors may cause the optimization problem to become infeasible. In this case, some technique has to be applied to drive the system state back to a feasible region. There are different approaches for this purpose, some of which will be briefly discussed in this section.

Initially, one must differentiate between two types of constraints, according to (Alvarez and Prada 1997):

Physical constraints: those limits that can be never surpassed and are determined by the physical functioning of the system. For instance, a valve cannot be opened more than 100%.

Operating constraints: those limits fixed by the plant operator. These limits, which are more restrictive than the physical constraints, define the band within which the variables are expected to be under normal operating conditions.

The physical constraints are also denominated hard constraints, given that they cannot be relaxed. In contrast, the operating constraints are called soft constraints.

(Alvarez and Prada 1997) describe a relaxation procedure that can be applied either to the controls or to the system outputs. The control-related approach consists of relaxing the operating constraints on the control amplitude or rate of change according to a priority schedule. The output-related approach consists of relaxing the operating constraints on the output amplitude or modifying the time interval where such constraints are imposed within the prediction horizon.

More sophisticated infeasibility handling techniques are described in (Rawlings and Muske 1993) and (Scokaert and Rawlings 1999):

Minimal time approach: An algorithm identifies the smallest time, $\kappa(x)$, which depends on the current state x, beyond which the state constraint can be satisfied over an infinite horizon. Prior to time κ, the state constraint is ignored, and the control law enforces the state constraint only after that time. An advantage of this method is that it leads to the earliest possible constraint satisfaction. Transient constraint violations, however, can be large.

Soft-constraint approach: Violations of the state constraints are allowed, but an additional term is introduced in the cost function to penalize the constraint violation.

The present work employs a gradual output constraint relaxation procedure, which consists of progressively relaxing the constraints until the optimization problem becomes feasible. It is worth noting that, by forcing the relaxations to be made on the output variable, the algorithm always produces control actions that are within the physical constraints for the plant.

For comparison, the standard approach for infeasibility handling employed by the quadratic programming solver available in the Matlab environment (`quadprog` function) is also investigated. In this case, when infeasibility occurs, the algorithm delivers a solution that minimizes the maximum distance to the violated constraint boundaries. Since no priorities are ascribed to the constraints, this solution may violate the control variable limits (related to either amplitude or rate of change), which, in the simulation scenario studied in this paper, are physical constraints. As will be seen in the simulation results, the consequences of adopting such an approach can be catastrophic.

4. Methodology

4.1 Plant model

The simulations carried out in this work concerned the dynamics of the Feedback Magnetic Levitation System©, which is depicted in Figure 2. The infrared photo-sensor is assumed to be linear in the required range of operation, yielding a voltage y that is related to distance h as $y = \gamma h + y_0$, where the gain $\gamma > 0$ and the offset y_0 are such that $y \in (-2V, +2V)$. Current i is regulated by an inner control loop, and is linearly related to the input voltage u as $i = ru + i_0$ with $r > 0$ and $i_0 > 0$. The working excursion of u is limited between $-3V$ (corresponding to a null coil current) and $+5V$ (saturation value). Rates of change larger than $50V/s$ for u cannot be implemented by the current driver along its entire working range.
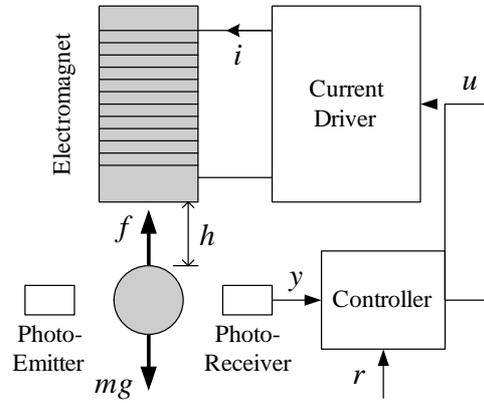
Figure 2. Main components of the control loop. The attraction force f is related to i and h in the form $f = Ki^2/h^2$, where $K > 0$ is an electromechanical conversion gain.

The dynamics of the vertical movement of the suspended sphere can be modelled by the following equation:

$$m\frac{d^2h}{dt^2} = mg - K\frac{i^2}{h^2} \tag{10}$$

where $K > 0$ is an electromechanical conversion gain, m is the mass of the sphere, g is the acceleration of gravity, and i is the coil current. As discussed in (Fama *et al.* 2005) and (Galvão *et al.* 2003), in view of the sensor and current driver characteristics, the model can be realized in state-space form as

$$\dot{x}_1 = x_2, \quad \dot{x}_2 = \gamma g - \frac{K(ru + i_0)^2\gamma^3}{m(x_1 - y_0)^2} \tag{11}$$

where $x = [y, \ dy/dt]^T$.

By using a first-order Taylor expansion around a given equilibrium point $\bar{x} = [\bar{y}, \ 0]^T$, a linearized model can be written as

$$\dot{\tilde{x}} = \begin{bmatrix} 0 & 1 \\ \alpha & 0 \end{bmatrix} \tilde{x} + \begin{bmatrix} 0 \\ -\beta \end{bmatrix} \tilde{u} \tag{12}$$

where $\alpha = 2\gamma g(\bar{y} - y_0)^{-1}$, $\beta = 2r\gamma^2(\bar{y} - y_0)^{-1}\sqrt{m^{-1}Kg}$ and the tilde denotes deviations from the equilibrium.

The following values for the physical model parameters were experimentally determined in (Grimm 2002): $m = 2.12 \times 10^{-2}$kg, $g = 9.8$m/s^2, $y_0 = -7.47$V, $\gamma = 328$V/m, $i_0 = 0.514$A, $r = 0.166$A/V, $K = 1.2 \times 10^{-4}$Nm^2/A^2.

The predictive control law was based on the model linearized around the center of the working range of the position sensor ($\bar{y} = 0$). A $5ms$ sampling period was adopted, relying on a previous study (Galvão *et al.* 2003) concerning the digital control of the system. Assuming that a zero-order hold will keep the control signal constant between sampling

instants (Hemerly 2000), the model matrices resulting after linearization and discretization are

$$A = \begin{bmatrix} 1.0109 & 0.0050 \\ 4.3773 & 1.0109 \end{bmatrix}, \quad B = \begin{bmatrix} -0.0144 \\ -5.7552 \end{bmatrix}, \quad C = \begin{bmatrix} 1 & 0 \end{bmatrix} \tag{13}$$

4.2 Simulation scenarios

All simulations were carried out in the Matlab 6.5/Simulink environment by using the nonlinear differential equations describing the system dynamics. A specific Matlab S-function was written to implement the predictive control law. The Quadratic Programming problem was solved by using the `quadprog` function of the Matlab Optimization Toolbox.

Appropriate prediction and control horizons were chosen on the basis of a previous paper (Fama *et al.* 2005), in which the authors determined that a prediction horizon $N = 20$ and a control horizon $M = 4$ produce a good compromise between speed of response and damping. Moreover, the control weight was set to $\rho = 10$ as recommended in (Fama *et al.* 2005) to achieve good rejection of measurement noise. The output constraints were set to $y_{min} = -0.01$V and $y_{max} = +0.01$V.

Two different simulation scenarios were considered in the study.

a)Starting from an infeasible point, without noise. In this first case, the sensor was assumed to be ideal (no measurement noise) and the initial conditions were set to $y = -0.1$V and $\dot{y} = 0$. The initial position is such that it violates the constraints, and thus the system starts at an infeasible point.

b)Starting from a feasible point, with noise. In this second case, the initial conditions were set within the feasible region ($y = 0$ and $\dot{y} = 0$) and white Gaussian noise with zero mean and variance of 1.6×10^{-5}V was added to the sensor measurements. In addition, since there is only a position sensor at the actual magnetic levitator, the speed was estimated from the position measurements by a filter with transfer function $100s/(s + 100)$.

In order to compensate the fact that the `quadprog` function may generate control actions outside the operational limits in infeasibility situations, an amplitude saturator and a rate limiter were introduced at the controller output, so that the control applied to the system is in agreement with the physical limits.

A constant-step relaxation scheme applied to the output constraints was compared with the default algorithm for infeasibility handling implemented in the `quadprog` function. In both simulation scenarios, the relaxation step was set to 0.05V for both the positive and negative output constraints (added to the positive constraint and subtracted from the negative one).

5. Results and discussion

5.1 Starting from an infeasible point, without noise

In this simulation scenario, the purpose consists of investigating the recovery from an initial infeasible point. No noise was added to the position measurements. The reference value for the sensor output was maintained at 0, but the initial condition was set to a position corresponding to $y = -0.1$V with null speed. It is worth noting that negative sensor measurements correspond to positions above the central line of the apparatus. Fig. 3a shows that the scheme with relaxation of output constraints deals with the infeasibility problem in a satisfactory manner, leading the system to the desired setpoint. In contrast, the default approach without relaxation leads to divergence (i.e. the suspended ball moves away from the magnetic core and falls).
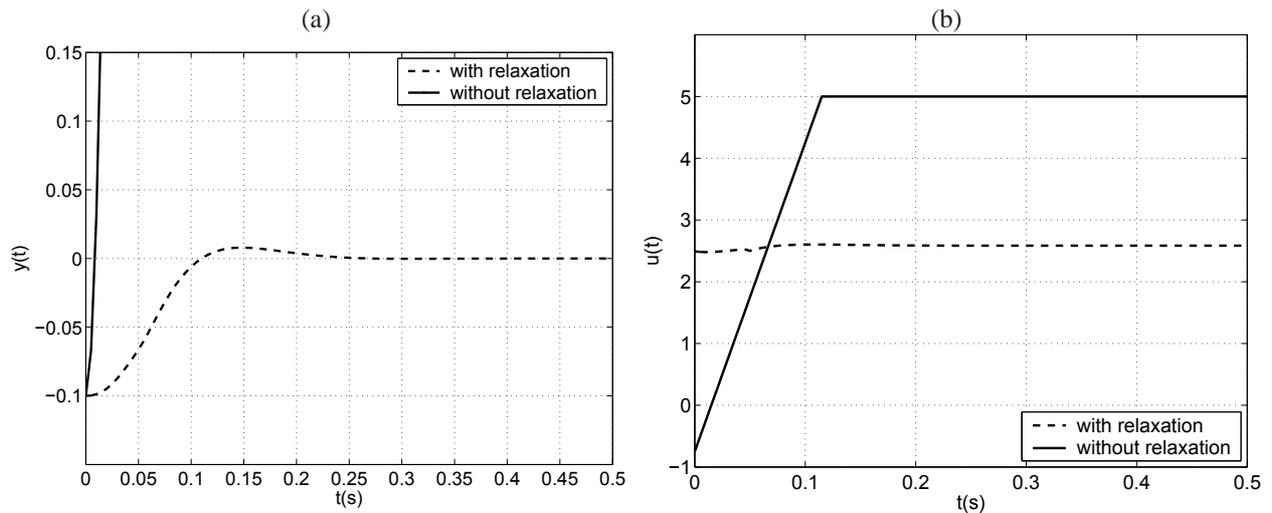
Figure 3. (a) Output and (b) control signals obtained in the simulation starting from an infeasible initial condition.

Figure 3b clarifies the action of the controller without the policy of constraint relaxation. Since the initial conditions violate the constraints, the controller applies a very small control signal (i.e., a very small current in the magnet coil) in the beginning and the ball starts to fall rapidly toward the feasible region. However, when the controller tries to recover the ball from its fall, the control action is limited, first by the rate of variation of the current (until approximately $0.1s$) and then by the upper bound on the current. As a result, the controller cannot prevent the ball from falling.

Finally, Fig. 4 demonstrates that the number of relaxations needed to circumvent the infeasibility problem is quite small, showing that the computational overhead involved in this approach is not significant. Also, it can be seen that the relaxations occur mostly when they are actually needed (when the constraint violation is bigger), and no more than the necessary. In fact, since the initial violation is of $-0.09V$ and the relaxation step is $0.05V$, only two relaxations are employed at the initial instant.
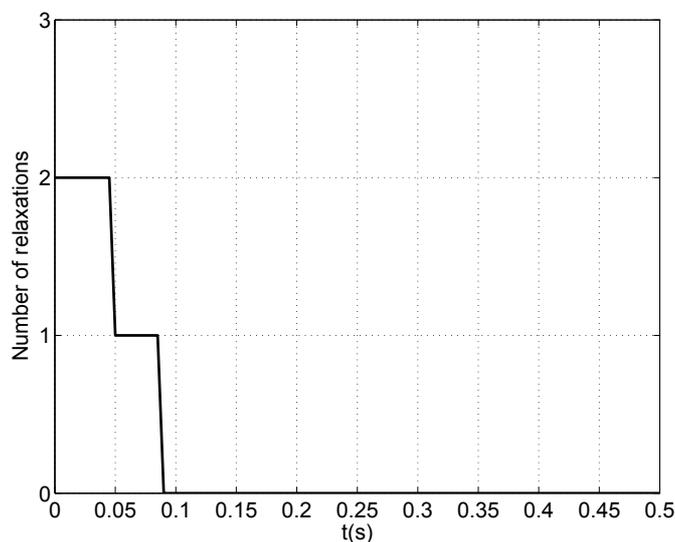
Figure 4. Number of relaxations at each time step for the first simulation scenario.

5.2 Starting from a feasible point, with noise

In this case, the simulation was carried out with the system starting from the reference value, $y = 0$V, which, of course, respects the constraints. White Gaussian noise was introduced at the sensor output in order to simulate measurement noise. Since there is no speed sensor, the velocity is estimated by the filtered derivative of the position.

Again, the performance obtained with output constraint relaxation is superior, as shown in Fig. 5a. As can be seen, the noise leads the system controlled without relaxation of constraints to diverge (the ball falls), while the one endowed with relaxation of constraints maintains the output around the reference value. It is important to note, however, that the relaxation of constraints cannot avoid the output oscillations, which occasionally violate the constraints. As in the

previous simulation, the control action of the approach without output constraint relaxation saturates the rate limiter and hits the upper bound for the current as shown in Fig. 5b.
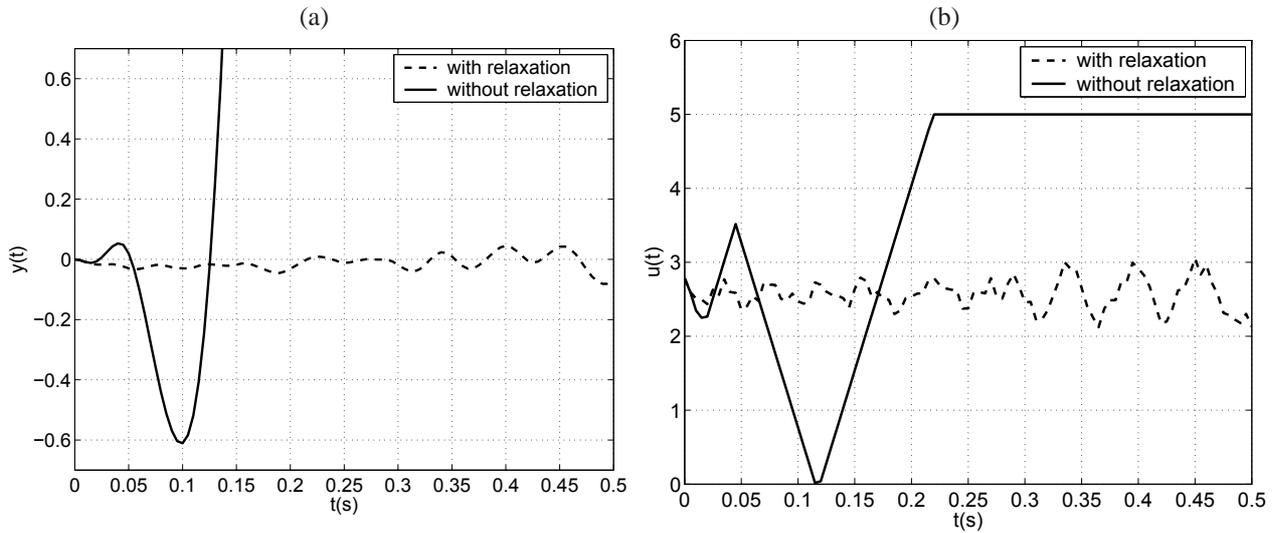
Figure 5. (a) Output and (b) control signals obtained in the simulation with measurement noise.

Finally, Fig. 6 illustrates the persistent acting of the relaxation algorithm every time that a violation occurs (or is predicted to occur) because of the noise. It is important to observe, however, that only one or two relaxation steps are enough to bring the system back to a feasible region in most cases.
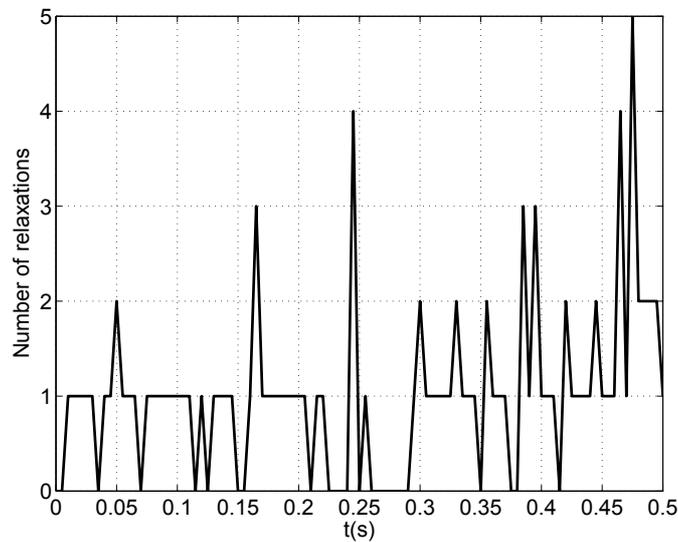
Figure 6. Number of relaxations at each time step for the second simulation scenario.

6. Conclusion

The results obtained in this work show that a simple policy of constraint relaxation in an MPC controller for a magnetic levitator can be quite benefic in comparison with the default approach implemented in a commercial optimization software. The study comprised two different situations: system starting from an infeasible point without noise and starting from a feasible point with noise. In both cases, the solution yielded by the approach without relaxation of constraints diverged, i.e., the suspended sphere fell down. In contrast, the scheme with relaxation of constraints was always capable of maintaining the plant working in a band around the setpoint. It is worth noting that the extra computational effort involved in the relaxation procedure was not significant, as seen from the small number of relaxations required in the process.

Such positive results motivate additional investigations concerning different techniques of constraint relaxation to circumvent infeasibility problems arising in the predictive control of magnetic levitation systems. Further research is needed to assess the benefits and disadvantages of each technique in terms of speed of recovery from initial infeasibility

conditions and regulation performance in the presence of disturbances and measurement noise.

7. Acknowledgements

8. References

Alvarez, T. and Prada, C., 1997, "Handling infeasibilities in predictive control", Computers in Chemical Engineering, Vol. 21, pp. S577–S582.

Camacho, E.F., Bordons, C., 1999, Model Predictive Control. Springer-Verlag. London.

Fama, R.C., Lopes, R.V. Milhan, A.P. Galvão, R.K.H., Lastra B.A.D., 2005, "Predictive control of a magnetic levitation system with explicit treatment of operational constraints", Proceedings of the 18th International Congress of Mechanical Engineering, Ouro Preto, MG, (paper 0560).

Galvão, R.K.H., Yoneyama, T., Araújo, F.M.U. and Machado, R.G., 2003, "A simple technique for identifying a linearized model for a didactic magnetic levitation system", IEEE Transactions on Education, Vol. 46, No. 1, pp. 22–25.

Grimm, C., 2002, "Um controlador digitalmente assistido para um sistema de levitação magnética", Master's thesis. ITA. São José dos Campos.

Hemerly, E.M., 2000, " Controle por Computador de Sistemas Dinâmicos", 2a ed.. Edgard Blücher. São Paulo.

Holmer, P., 2003, "Faster than a speeding bullet train", IEEE Spectrum, Vol. 40, No. 8, pp. 30–34.

Kim, W.J. and Trumper, D.L., 1998, "High-precision magnetic levitation stage for photolithography", Precision Engineering – Journal of the International Societies for Precision Engineering and Nanotechnology, Vol. 22, No. 2, pp. 66 – 77.

Maciejowski, J.M., 2002, "Predictive Control with Constraints", Prentice Hall. Harlow, England.

Masuzawa, T., Ezoe, S., Kato, T. and Okada, Y., 2003, "Magnetically suspended centrifugal blood pump with an axially levitated motor", Artificial Organs, Vol. 27, No. 7, pp. 631 – 638.

Rawlings, J.B. and Muske, K.R., 1993, "The stability of constrained receding horizon control", IEEE Transactions on Automatic Control, Vol. 38, No. 10, pp. 1512–1516.

Scokaert, P.O.M. and Rawlings, J.B., 1999, "Feasibility issues in linear model predictive control", AIChE Journal, Vol. 45, No. 8, pp. 1649–1659.

Varvella, M., Calloni, E., Di Fiore, L., Milano, L. and Arnaud, N., 2004, "Feasibility of a magnetic suspension for second generation gravitational wave interferometers", Astroparticle Physics, Vol. 21, No. 3, pp. 325 – 335.

9. Responsibility notice

The author(s) is (are) the only responsible for the printed material included in this paper